Solvent Effect on the Reactivity of *cis*-Platinum (II) Complexes: A Density Functional Approach

PUBALEE SARMAH, RAMESH C. DEKA

Department of Chemical Sciences, Tezpur University, Napaam, Tezpur 784028, Assam, India

Received 28 October 2007; accepted 9 January 2008
Published online 6 March 2008 in Wiley InterScience (www.interscience.wiley.com).
DOI 10.1002/qua.21635

ABSTRACT: The structure and chemical reactivity of some selected *cis*-platinum(II) complexes, including clinically used drug molecules, cisplatin, carboplatin, and oxaliplatin are investigated using density functional theory (DFT) calculations. Calculated geometries of the complexes are in agreement with their available X-ray data. The global and local reactivity descriptors, such as hardness, chemical potential, electrophilicity index, Fukui function, and local philicity are calculated to investigate the usefulness of these descriptors for understanding the reactive nature and reactive sites of the complexes. Inclusion of solvent effect shows that both global and local descriptors change the trend of reactivity with respect to their trend in the gas phase. The stability of the complexes increases with the inclusion of water molecules. Simple regression analysis is applied to build up a quantitative structure-activity relationship (QSAR) model based on DFT derived electrophilicity index for the Pt(II) complexes against A2780 human ovarian adenocarcinoma cell line to establish the importance of the descriptor in predicting cytotoxicity. Int J Quantum Chem 108: 1400–1409, 2008

Key words: chemical reactivity; drug molecules; DFT; solvent effect; QSAR

Introduction

Metal ions and metal coordination compounds are known to affect cellular processes among which most important metal used in the treatment of cancer over the last decade has been platinum. The successful development of metal-containing anticancer drugs began with *cis*-diamminedichloroplatinum(II), clinically known as cisplatin [1], the anticancer activity of which was discovered by Rosenberg et al. [2]. Cisplatin is a paradigm for the treatment of testicular and ovarian cancer [3–5]. Although the nephrotoxicity of cisplatin can be repressed, other toxic side effects (such as nausea, ear damage, or vomiting) of its

Correspondence to: R. C. Deka; e-mail: ramesh@tezu.ernet.in
Contract grant sponsors: Council of Scientific and Industrial Research (CSIR), Department of Science and Technology (DST).

treatment and intrinsic and acquired cellular resistance have stimulated research toward developing analogs of cisplatin with lesser toxic effects. The second generation platinum drug, carboplatin has received worldwide approval in a routine clinical use [6]. The observed pharmacokinetic differences between cisplatin and carboplatin depend on the slower rate of conversion of carboplatin to the reactive species. Replacement of the chloride groups in cisplatin by cyclobutanedicarboxylate ligand significantly diminished the nephrotoxic effects of the formed carboplatin without affecting its antitumor activity. Other drugs containing oxygen ligands as leaving groups include oxaliplatin and nedaplatin [6]. Unfortunately, these mononuclear drugs also suffer from drug resistance and other side effects [3, 4]. Dinuclear Pt(II) complexes (third generation) have been especially designed to cause a different cellular response than cisplatin, reducing the risk of both cross-and intrinsic resistance [3, 7].

Platinum anticancer drugs bind to DNA, forming a variety of intrastrand and interstrand adducts, the most abundant of which are 1,2-intrastrand cross-links between the N7 atoms of two adjacent guanine bases [4]. It is believed that cisplatin and some of its analogs are activated before eliciting biological effects via substitution of the leaving group to form a reactive aquated platinum species in solution [8–11]. There are also evidences for the direct attack of the cisplatin and its analogs to the 5′-GMP (5-guanosine monophosphate) [12–13]. Studies on the interaction of carboplatin with DNA indicate that the reaction proceeds via ring-opening in carboplatin and subsequent binding with DNA constituents. However, azol bridged dinuclear platinum(II) complexes react with DNA by a mechanism that is distinct from cisplatin and its analogues [14, 15].

In recent years, there has been an increasing interest in density functional theory (DFT), both in its conceptual and computational aspects [16–19]. In computational DFT, the molecular properties of a system are calculated with better quality/cost ratio using electron density as a fundamental property. On the other hand, a series of reactivity descriptors have been introduced within the context of conceptual DFT. Global reactivity descriptors namely, global hardness (η) [20] and global softness (S), electronegativity (χ) and chemical potential (μ) [21], and electrophilicity index (ω) [22] represent properties of a molecule as a whole. Other type of descriptors are local reactivity descriptors that include local softness ($s(\vec{r})$) [23], Fukui functions (FFs) ($f(\boldsymbol{r})$)[24] etc., which have attracted considerable interests to describe the relative reactivity and site selectivity in chemical reactions. The first application of DFT based reactivity descriptors to a biological system was applied to inorganic model systems for arsenate reductase and phosphatase [25]. Recently, Beck [26] has calculated local reactivity descriptors, FFs for a number of drugs and agrochemicals to investigate whether maxima of these functions can be related to the sites of metabolism.

Nowadays, theoretical calculations of molecular and electronic structure represent a valuable complement to experiment to elucidate structure-activity relationships. Modeling of quantitative-structure-activity relationship (QSAR) by using density functional descriptors has been recently reviewed by Chattaraj et al. [27]. Many studies were devoted to this field and well documented [28–31]. The importance of electrophilicity index in understanding the toxicity and biological activity of various organic molecules has been demonstrated and found that it is suitable in effectively describing the toxicity and biological activity [28–33].

Over the past few years, many theoretical studies have been performed on hydrolysis of cisplatin and its analogs [34, 35] and electronic structure calculations on drug-nucleoside complexes [36–39]. To study the reaction pathway followed by the drug molecules and their binding properties, it is important to understand the reactive nature of these molecules. Although several studies have been reported regarding the usefulness of DFT based descriptors in structure-activity/toxicity/property analyses of organic molecules, to the best of our knowledge, systematic studies on the cytotoxicity of platinum complexes have not yet been reported.

In this article, global properties are calculated to study the reactivity for a number of clinically used platinum anticancer drugs including some model *cis*-Pt (II) complexes with varying carrier and the leaving groups. We also calculated the FF and local philicity of these drug molecules to establish the importance of these descriptors in describing the reactive sites of the molecules for which metabolites are known. The effect of solvation on the reactivity of the complexes is analyzed. Further, the cytotoxicity values expressed as log (IC_{50}^{-1}) of the Pt (II) complexes against A2780 human ovarian adenocarcinoma cell line are modeled by the linear regression analysis using the DFT-based global reactivity descriptors ω to analyze the usefulness of electrophilicity in describing the biological activity of these molecules.

Methods

THEORETICAL BACKGROUND

In theoretical chemistry, the chemical potential (μ) is identified as the negative of the electronegativity (χ) by Iczkowski and Margrave [40] and defined as

$$\chi = -\mu = -\left(\frac{\partial E}{\partial N}\right)_{\upsilon(\vec{r})} \tag{1}$$

and hardness (η) [20] of an electronic system is defined as the second derivative of total energy (E) with respect to the number of electrons (N) at constant external potential, $\nu(\vec{r})$,

$$\eta = \frac{1}{2}\left(\frac{\partial^2 E}{\partial N^2}\right)_{\nu(\vec{r})} = \frac{1}{2}\left(\frac{\partial \mu}{\partial N}\right)_{\nu(\vec{r})}. \tag{2}$$

Using the finite difference approximation, global hardness and chemical potential can be approximated as

$$\eta = \frac{\mathrm{IP} - \mathrm{EA}}{2} \tag{3}$$

$$\mu = -\left(\frac{\mathrm{IP}+\mathrm{EA}}{2}\right) \tag{4}$$

where IP and EA are the first vertical ionization potential and electron affinity, respectively, of the chemical system.

Further approximation using Koopmans' theorem [41], the above parameters can be expressed by taking IP and EA as negative of the HOMO and LUMO energies,

$$\mu = \frac{E_{\mathrm{LUMO}} + E_{\mathrm{HOMO}}}{2} \tag{5}$$

and

$$\eta = \frac{E_{\mathrm{LUMO}} - E_{\mathrm{HOMO}}}{2} \tag{6}$$

where E_{LUMO} is the energy of the lowest unoccupied molecular orbital and E_{HOMO} is the energy of the highest occupied molecular orbital.

Parr et al. [22] introduced the global electrophilicity index (ω) in terms of chemical potential and hardness as

$$\omega = \frac{\mu^2}{2\eta}. \tag{7}$$

According to this definition, ω describes the electrophilic power of a molecule.

The FF, [24] a frontier MO reactivity index is by far the most important local reactivity index and defined as

$$f(r) = \left[\frac{\delta \mu}{\delta \nu(r)}\right]_N = \left[\frac{\delta \rho(r)}{\delta N}\right]_{\nu(r)}. \tag{8}$$

Mendez and Gazquez [42] and Yang and Mortier [43] introduced a procedure to obtain information about *f(r)*. This procedure condenses the values around each atomic site into a single value that characterizes the atom in the molecule. With this approximation, the condensed FF becomes

$$f_k^+ = [q_k(N+1) - q_k(N)]$$

(for nucleophilic attack on the system) (9a)

$$f_k^- = [q_k(N) - q_k(N-1)]$$

(for electrophilic attack on the system) (9b)

$$f_k^0 = \frac{1}{2}[q_k(N+1) - q_k(N-1)]$$

(for radical attack on the system) (9c)

where $q_k(N)$, $q_k(N+1)$, and $q_k(N-1)$ are the charges of the kth atom for N, $N+1$ and $N-1$ electron systems, respectively.

Recently, Chattaraj et al. [44] have defined a generalized concept of philicity associated with a site k in a molecule as

$$\omega_k^\alpha = \omega f_k^\alpha \tag{10}$$

where $\alpha = +, -$, and 0 represent nucleophilic, electrophilic, and radical attacks, respectively.

COMPUTATIONAL DETAILS

All the density functional calculations were carried out using the DMol^3 program [45]. The complexes were subjected to full geometry optimization

TABLE I
Platinum(II) complexes.

Complexes	no.
cis-diamminedicholrideplatinum(II) (cisplatin)	1
cis-diammine(1,1′-cyclobutanedicarboxylato)platinum(II) (carboplatin)	2
cis-(1,1′-cyclobutanedicarboxylato)ethylenediamineplatinum(II)	3
cis-[(1*R*,2*R*)-1,2-diaminocyclohexane]oxalatoplatinum(II) (oxaliplatin)	4
cis-[(1*R*,2*R*)-1,2-diaminocyclohexane]malonatoplatinum(II)	5
cis-dichloride[(1*R*,2*R*)-1,2-diaminocyclohexane]platinum(II)	6
cis-(1,1′-cyclobutanedicarboxylato)[(1*R*,2*R*)-1,2-diaminocyclohexane]platinum(II)	7

using double numerical with polarization (DNP) basis set [45] in combination with three generalized gradient approximation (GGA) exchange-correlation functionals BLYP, BOP, and HCTH. The DNP basis is comparable to Gaussian 6-31G** basis set [46–48]. However, it is believed to be much more accurate than a Gaussian basis set of the same size. DMol^3 has a facility that applies scalar relativistic corrections to this basis set. We performed all electron calculations, including relativistic effects for all complexes. The most popular exchange-correlation functional BLYP is the combination of the exchange functional developed by Becke [49] with the gradient corrected correlation functional by Lee et al. [50]. BOP is the combination of Becke [49] exchange and one-parameter progressive OP [51] correlation functionals. In HCTH both exchange and correlation parts were developed by Hamprecht et al. [52]. The minimized structures were confirmed as minima via harmonic vibrational frequency calculations. The global reactivity descriptors chemical potential, hardness, and electrophilicity index were calculated for all the systems using Eqs. (5)–(7), respectively. The Hirshfeld [53] population analysis (HPA) was used to calculate the FF. While comparing the calculated geometrical parameters of the drug molecules with the experimental data, we found that the BLYP/DNP calculations worked better than BOP/DNP and HCTH/DNP calculations. Hence, we performed BLYP/DNP level calculations to study the effect of solvent (water) using conductor-like screening model (COSMO)[54] as incorporated into the DMol^3 program with dielectric constant of 78.4. The FF (f^+) and local philicity (ω_k^+) were calculated for all atoms of the drug molecules using Eqs. (9) and (10), respectively. One parameter QSAR [55] was performed using least square error estimation method [56] to calculate and compare the cytotoxicity (log IC_{50}^{-1}) of the complexes.

Results and Discussion

STRUCTURE

The list of the studied *cis*-platinum(II) complexes are tabulated in Table I. The gas phase optimized structures obtained from BLYP/DNP level calculations for the platinum (II) complexes are shown in Figure 1. Selected bond lengths and bond angles of the complexes, both in gas and solvent phases are

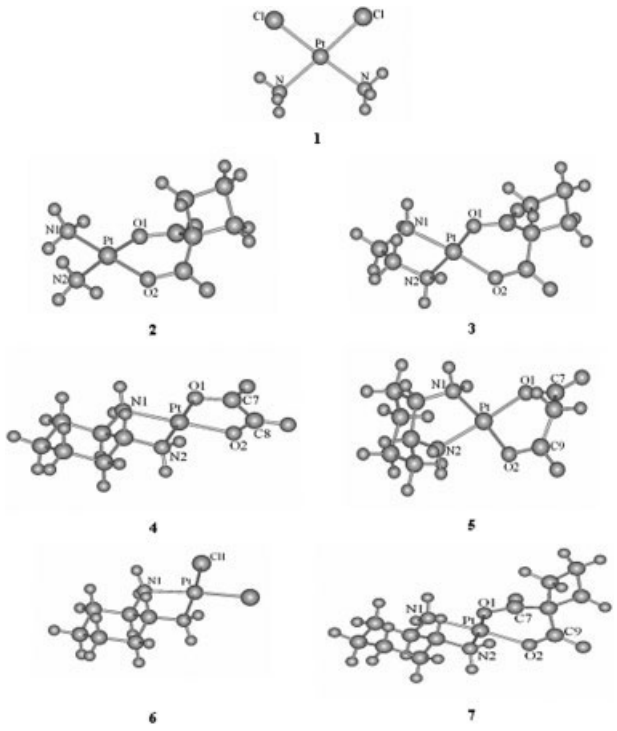

FIGURE 1. Optimized structures for the *cis*-Pt(II) complexes with numbering of selected atoms obtained from BLYP/DNP calculations.

provided in Table II. The optimized geometry of cisplatin (1) has a square-planar structure in both gas and solvent media, which is in agreement with X-ray crystal structure reported by Milburn and Truter [57]. The calculated Pt—Cl and Pt—N bond lengths in gas phase are 2.32 Å and 2.11Å, respectively in accordance with their experimental values (Table II). In the gas phase calculations the N—Pt—N angle (97.1°) deviates slightly more from its experimental value (87°±1.5°). The Cl—Pt—Cl angle is also larger than its experimental value by about 5°–6°. Similar deviation of bond angles in cisplatin was reported in theoretical studies performed by Wysokinski and Michalska [58]. These higher values could be due to the intramolecular N—H· · ·Cl interaction of cisplatin in the gas phase, which opens up both the N—Pt—N and Cl—Pt—Cl angles. Inclusion of solvent effect decreases the N—Pt—N and Cl—Pt—Cl angles from their gas phase values to 89.2° and 93.9°, respectively.

In carboplatin (2) chlorine atoms are replaced by cyclobutanedicarboxylate groups where two ammine groups are in the cis position. The planar environment of the platinum atom and the boat conformation for the six-membered chelate ring obtained from gas phase and solvent phase calculations are in agreement with the X-ray diffraction data [59, 60] (Table II). Our calculations both in gas and solvent media predict a slightly puckered structure of cyclobutane ring which is also supported by the experimental data. The Pt—N bond length is slightly shorter than that of cisplatin. This is in consistent with the results obtained from different theoretical methods by Wysokinski and Michalska [58]. The geometrical parameters of the complex 3, in which carrier ligands NH_3 of carboplatin are replaced by ethylenediamine, are compared with that of carboplatin in Table II. For this complex, again we have obtained boat conformation of the six-membered chelate ring with a puckered structure of cyclobutane ring.

Oxaliplatin (4) has (1*R*,2*R*)-1,2-diaminocyclohexane (DACH) as a carrier ligand and oxalate (OX) as a leaving ligand. From complex 5–7, keeping DACH as a carrier ligand, the leaving ligands are varied as malonato (MAL), chloride and 1,1′-cyclobutanedicarboxylato (CBDC), respectively. The bond lengths and bond angles of oxaliplatin obtained from gas and solvent phases are close to its X-ray crystal structure data [61]. In both the phases, chair configuration of the cyclohexane ring with two amino groups in equatorial positions is found in accordance with the experimental results. The geometry of complex 5 is compared with the experimental result [61] in Table II. In this compound, the cyclohexane ring has chair conformation whereas in direct contrast, the malonato ligand shows a boat conformation for the six membered Pt—O—C—C—C—O ring. This is in good agreement with the experimental data. For compounds 6 and 7, again we have found cyclohexane ring with chair conformation whereas the carboxylato group of CBDC in 7 has boat conformation. Their geometrical parameters are comparable with the X-ray data of oxaliplatin [61]. Thus, it is observed that our calculated geometries for all the complexes are in good agreement with their experimental data. However slightly higher values of bond lengths for all most all the cases are due to the BLYP exchange correlation functional that is known to overestimate the bond lengths [62, 63].

REACTIVITY

Global Descriptors

The gas phase values of chemical hardness (η), chemical potential (μ), and electrophilicity index (ω) computed using DNP basis set in connection with the three exchange-correlation functionals for the compounds are given in Table III. It is observed that all the methods predict similar trend for these descriptors except the electrophilicity trend for oxaliplatin and complex 5 at BLYP/DNP level. According to the maximum hardness principle (MHP) [64, 65], the most stable structure has the maximum hardness. Thus in gas phase, complex 7 is found to be the most stable structure. This complex has the minimum value of ω and maximum value of μ and hence the least reactive whereas cisplatin (1) has the maximum ω and minimum μ values and is the most reactive among the complexes with a minimum value of η. The higher reactivity of cisplatin agrees well with most of the platinum drug literatures, for which the toxicity of the molecule is more.

The variation of hardness calculated with BLYP/DNP level for the complexes is shown in Figure 2. The leaving ligands of each complex are also displayed in the plot. It is observed that the compounds having chloride groups (1,6) as leaving ligand exhibit higher reactivity whereas the CBDC as leaving groups make the complexes harder.

The calculated values of global reactivity descriptors, η, μ, and ω from the BLYP/DNP method in solvent medium are presented in Table IV. The reactivity trend of the molecules in gas phase

TABLE II

Selected bond lengths (in Å) and angles (in deg) calculated for all complexes at BLYP/DNP level.

	X-ray (1)	1		X-ray (2)	2	3		X-ray (4)	X-ray (5)	4	5	6	7
Pt—Cl	2.33 ± 0.01	2.32	Pt—N1	2.01	2.10	2.09	Pt—O1	2.01	2.02	2.00	2.01		2.00
		(2.33)			(2.07)	(2.07)				(2.04)	(2.03)		(2.04)
Cl—Pt—Cl	91.9 ± 0.3	96.8	Pt—O1	2.02	2.00	2.00	Pt—N1	2.06	2.03	2.08	2.07	2.07	2.07
		(93.9)			(2.03)	(2.04)				(2.06)	(2.06)	(2.07)	(2.06)
Pt—N	2.01 ± .04	2.11	O1—Pt—N1	88.2	80.6	90.3	O1—C7	1.21	1.24	1.27	1.31		1.32
		(2.08)			(88.4)	(82.9)				(1.25)	(1.29)		(1.29)
N—Pt—N	87 ± 1.5	97.1	N1—Pt—N2	93.6	103.1	84.1	O2—C8	1.32		1.35			
		(89.2)			(91.4)	(93.7)				(1.32)			
			O1—Pt—N2	177.9	175.8	173.9	O2—C9		1.35		1.34		1.34
					(179.9)	(176.2)					(1.32)		(1.32)
			O1—Pt—O2	88.9	95.9	95.4	Pt—Cl1					2.32	
					(91.5)	(89.7)						(2.35)	
							O2—Pt—O1	82.5	90.3	84.3	96.0		94.9
										(82.3)	(91.8)		(89.2)
							N1—Pt—O1	96.0	93.2	96.4	89.9		90.7
										(98.6)	(92.8)		(94.5)
							N2—Pt—O1	175.6	177.0	179.1	173.6		173.8
										(178.7)	(174.7)		(176.4)
							N1—Pt—O2	169.7	176.4	172.8	173.3		174.2
										(179.7)	(175.0)		(176.1)

Solvent phase values are in parenthesis.

TABLE III

Calculated hardness (η, in eV), chemical potential (μ, in eV), and electrophilicity index (ω, in eV) for all complexes in gas phase.

Complex	BLYP			BOP			HCTH		
	η	μ	ω	η	μ	ω	η	μ	ω
1	1.474	−3.491	4.134	1.485	−3.371	3.826	1.605	−3.627	4.098
2	1.714	−3.398	3.368	1.703	−3.263	3.126	1.813	−3.539	3.454
3	1.690	−3.165	2.964	1.682	−3.036	2.740	1.792	−3.336	3.105
4	1.629	−2.995	2.753	1.626	−2.870	2.533	1.776	−3.182	2.850
5	1.676	−3.034	2.746	1.683	−2.925	2.542	1.798	−3.209	2.864
6	1.504	−3.040	3.072	1.506	−2.931	2.852	1.626	−3.212	3.172
7	1.724	−2.999	2.608	1.716	−2.871	2.402	1.824	−3.158	2.734

changes with the inclusion of solvent medium. The variation of chemical hardness values of the complexes in both the media is shown in Figure 3. The higher values of hardness in solvent-phase indicate that all complexes display increased stabilization in this medium. However, only slight difference in hardness is observed for oxaliplatin (4). It is very interesting to note from Figure 3 that the most reactive complex changes from cisplatin (1) to oxaliplatin (4) in going from gas phase to solvent phase. On the other hand, solvent-phase calculations predict carboplatin (2) as the least reactive among the other platinum complexes in contrast to the gas phase calculations. The higher reactivity of oxaliplatin than that of other two clinically used drugs (2 and 4) is in agreement with the data reported by Baguley and co-workers [66]. They observed reactivity of some platinum anticancer drugs by measuring the half-life of binding to plasma proteins in vitro and found higher reactivity of oxaliplatin than that of cisplatin.

Figure 4 shows the variation of electrophilicity descriptors (ω) for all selected systems both in gas and solvent media. It is interesting to observe that complexes 1–3 have lower values of ω in solvent medium compared to their respective counterparts in the gas phase; however, this trend becomes reverse for complexes 4–7. This variation indicates that the presence of DACH as carrier groups (4–7) exhibited the highest electrophilicity values, which could be a reason behind higher cytotoxic effects of these complexes.

Local Descriptors

Local reactivity parameters describe the relative reactivity and site selectivity of chemical species. The nucleophilic attack at a particular site of a system represents the sites with maximum values

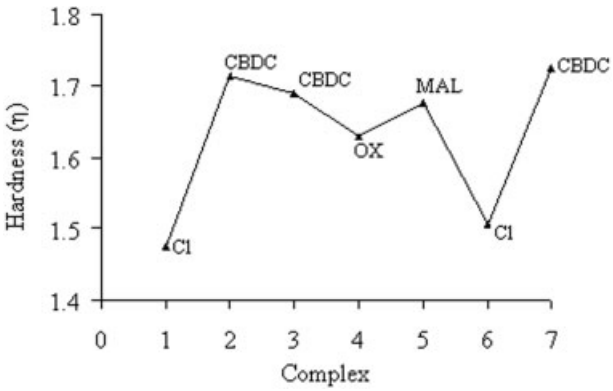

FIGURE 2. Variation of hardness of the molecules calculated at BLYP/DNP level. The leaving ligands of the complexes are also shown.

TABLE IV

Calculated hardness (η, in eV), chemical potential (μ, in eV) and electrophilicity index (ω, in eV) for all complexes in solvent phase at BLYP/DNP level.

Complex	BLYP/DNP		
	η	μ	ω
1	1.685	−3.618	3.884
2	1.973	−3.336	2.851
3	1.803	−3.101	2.666
4	1.638	−3.777	4.357
5	1.957	−3.407	2.966
6	1.668	−3.573	3.815
7	1.950	−3.536	3.748

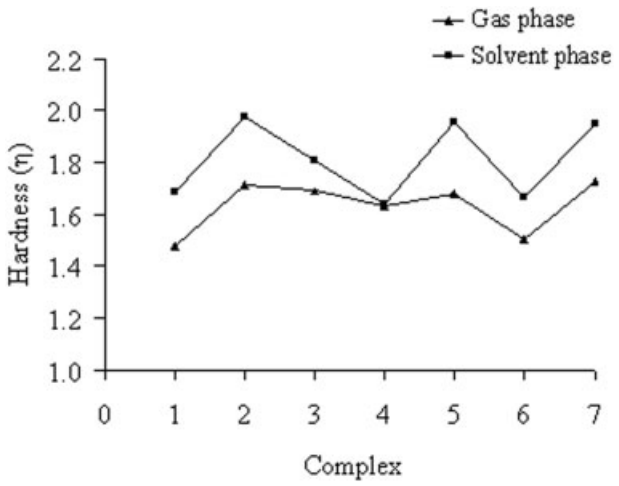

FIGURE 3. Variation of hardness of the molecules for both gas and solvent media.

of FF, f^+ and/or local philicity, ω^+. Similarly, electrophilic attack at a particular site of a system represents the sites with maximum values of FF, f^- and/or local philicity, ω^-. The platinum anticancer drug-DNA binding mechanism involves the nucleophilic attack at Pt atom. So, in the present study, f^+ and ω^+ values are calculated for all the atoms of the complexes both in gas and solvent media using the Hirshfeld Population Analysis scheme. As expected, in all the systems Pt sites are prone to nucleophilic attack with maximum values of f^+ and ω^+.

The gas phase and solvent phase values of f^+ and ω^+ of Pt atom in complexes (1–7) derived from BLYP/DNP method are presented in the Table V. It is seen from Table V that f^+ and ω^+ values of the Pt atoms of all most all the complexes in the solvent medium are larger than their gas phase values.

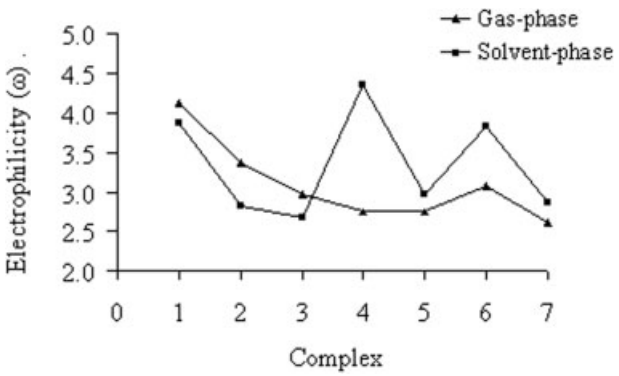

FIGURE 4. Variation of electrophilicity index of the molecules for both gas and solvent media.

TABLE V

Fukui function (f^+) and local philicity indices (ω^+) of Pt atom of the complexes both in solvent and gas phases calculated at BLYP/DNP level.

	f^+		ω^+	
System	Solvent phase	Gas phase	Solvent phase	Gas phase
1	0.272	0.210	1.056	0.868
2	0.245	0.162	0.691	0.546
3	0.242	0.145	0.645	0.430
4	0.089	0.126	0.388	0.347
5	0.274	0.150	0.813	0.412
6	0.260	0.196	0.992	0.602
7	0.236	0.132	0.885	0.344

Solvent phase derived f^+ value of oxaliplatin (4) does not follow the regular trend. However, for this complex ω^+ value in the solvent phase is higher than that of gas phase. These results indicate that the Pt atoms of the complexes in solvent phase are chemically softer than that of gas phase.

STRUCTURE-ACTIVITY ANALYSIS

The inhibitory activity (IC_{50}) values of the platinum complexes against A2780 human ovarian adenocarcinoma cell line was taken from the results reported by Osella and co-workers [67]. As usual, these data were changed to log IC_{50}^{-1} to be practical use in the QSAR analysis which is modeled by using a linear regression technique. Linear regression analyses were carried out for both solvent and gas phases by considering the experimental cytotoxic activity log IC_{50}^{-1} as a dependent variable and the DFT based global reactivity descriptors (ω) obtained from BLYP/DNP method as an independent variable. It is observed that in the gas phase ω fails to predict the cytotoxic activity of the complexes. In direct contrast, the ω values in the solvent phase could predict the cytotoxicity of the complexes indicating the importance of solvent model in the study of biomolecules. The modeled regression equation in the solvent phase is given by

$$\log IC_{50}^{-1} = -6.152 + 1.5659 \times \omega$$
$$N = 7,\ r^2 = 0.889,\ \mathrm{SD} = 0.389\ . \quad (11)$$

It is observed that the derived model accounts for the 88.9% variance in the experimental data

with a root-mean-square error (SD) of 0.389. Table VI lists the experimental and calculated cytotoxicity of the complexes. A plot between the experimental and calculated cytotoxicity values of the complexes (see Fig. 5) shows that the electrophilicity indices (ω) are capable of predicting the cytotoxicity in a reasonable way with a correlation coefficient (r) of 0.943. Thus, log IC_{50}^{-1} exhibits a reasonable correlation with electrophilicity which clearly indicates the fact that electrophilicity can be effectively used as descriptors in the prediction of cytotoxicity of platinum complexes.

Conclusions

Systematic theoretical calculations of *cis*-platinum (II) complexes both in gas and solvent phases have been carried out in order to assess their structure, stability, and reactivity. The geometrical parameters of the molecules computed using both gas and solvent phases agree well with the available experimental data. The reactivity sequences derived by calculating global hardness values are different in the gas phase and solvent medium. Global hardness values calculated in the solvent medium reproduced the experimental reactivity trend of cisplatin, carboplatin, and oxaliplatin. For complexes 1–3, the electrophilicity values in the solvent phase are smaller than that of the gas phase, whereas, the complexes 4–7 have higher values of electrophilicity in the solvent phase compared to their gas phase values. QSAR analysis performed using solvent phase derived electrophilicity values showed a good correlation with the experimental cytotoxicity values. Thus, these results indicate the significance of electrophilicity index in predicting structure-activity relationship of drug molecules.

TABLE VI

Experimental and solvent phase calculated cytotoxic activity (log IC_{50}^{-1}) values of the Cis-Pt(II) complexes against A2780 human ovarian adenocarcinoma cell line from BLYP/DNP level.

	log IC_{50}^{-1}		
system	observed[a]	calculated	residual[b]
1	−0.315	−0.070	−0.245
2	−2.036	−1.737	−0.300
3	−0.030	−0.178	0.149
4	−2.220	−1.977	−0.243
5	−0.798	−1.509	0.711
6	0.734	0.671	0.063
7	−0.419	−0.284	−0.135

[a] From reference 67. [b]Difference between the experimental and calculated values of cytotoxicity (log IC_{50}^{-1}).

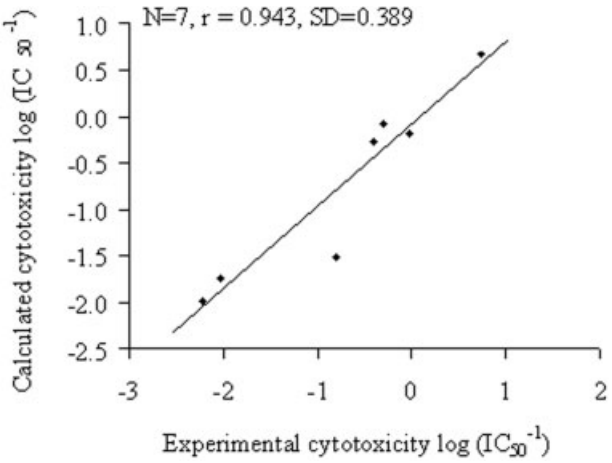

FIGURE 5. A plot between experimental and calculated cytotoxicity (log IC_{50}^{-1}) values of all *cis*-Pt(II) complexes against A2780 human ovarian adenocarcinoma cell line.

References

1. Rosenberg, B.; Van Camp, L. V.; Krigas, T. Nature (London) 1965, 205, 698.
2. Rosenberg, B.; Van Camp, L. V.; Trosko, J. E.; Mansour, V. H. Nature (London) 1969, 222, 385.
3. (a) Reedijk, J. Proc Natl Acad Sci USA 2003, 100, 3611; (b) Wang, D.; Lippard, S. J. Nat Rev Drug Discov 2005, 4, 307.
4. Jamieson, E. R.; Lippard, S. J. Chem Rev 1999, 99, 2467.
5. Wong, E.; Giandomenico, C. M. Chem Rev 1999, 99, 2451.
6. Lebwohl, D.; Canetta, R. Eur J Cancer 1998, 34, 1522.
7. Jakupec, M. A.; Galaski, M.; Keppler, B. K. Rev Physiol Biochem Pharmacol 2003, 146, 1.
8. Teo, B. K.; Eisenberg, P.; Reed, J.; Barton, J. K.; Lippard, S. J. J Am Chem Soc 1978, 100, 3225.
9. Miller, S. E.; House, D. A. Inorg Chim Acta 1989, 166, 189.
10. Bancroft, D. P.; Lepre, C. A.; Lippard, S. J. J Am Chem Soc 1990, 112, 6860.
11. Miller, S. E.; Gerard, K. J.; House, D. A. Inorg Chim Acta 1991, 190, 135.
12. Marcelis, A. T. M.; van Kralingen, C. G.; Reedijk, J. J Inorg Biochem 1980, 13, 213.
13. Eastman, A. Biochemistry 1983, 22, 3927.
14. Komeda, S.; Ohishi, H.; Yamane, H.; Harikawa, M.; Sakaguchi, K.; Chikuma, M. J Chem Soc Dalton Trans 1999, 17, 2959.
15. Komeda, S.; Lutz, M.; Spek, A. L.; Chikuma, M.; Reedijk, J. Inorg Chem 2000, 39, 4230.

16. Parr, R. G.; Yang, W. Density-Functional Theory of Atoms and Molecules; Oxford University Press: New York, 1989.
17. Parr, R. G.; Yang, W. Annu Rev Phys Chem 1995, 46, 701.
18. Geerlings, P.; De Proft, F.; Langenaeker, W. Adv Quantum Chem 1999, 33, 303.
19. Chermette, H. J Comput Chem 1999, 20, 129.
20. Parr, R. G.; Pearson, R. G. J Am Chem Soc 1983, 105, 7512.
21. Parr, R. G.; Donnelly, R. A.; Levy, M.; Palke, W. E. J Chem Phys 1978, 68, 3801.
22. Parr, R. G.; Szentpaly, L. V.; Liu, S. J Am Chem Soc 1922, 1999, 121.
23. Yang, W.; Parr, R. G. Proc Natl Acad Sci USA 1984, 82, 6723.
24. Parr, R. G.; Yang, W. J Am Chem Soc 1984, 106, 4049.
25. Roos, G.; Loverix, S.; De Proft, F.; Wyns, L.; Geerlings, P. J Phys Chem A 2003, 107, 6828.
26. Beck, M. E. J Chem Inf Model 2005, 45, 273.
27. Chattaraj, P. K.; Nath, S.; Maiti, B. In Computational Medicinal Chemistry for Drug Discovery; Tollenaere, J.; Bultinck, P.; Winter, H. D.; Langenaeker, W., Eds.; Marcel Dekker: New York, 2003; Chapter 11, pp 295.
28. Padmanabhan, J.; Parthasarathi, R.; Subramanian, V.; Chattaraj, P. K. Bioorg Med Chem 2006, 14, 1021.
29. Padmanabhan, J.; Parthasarathi, R.; Subramanian, V.; Chattaraj, P. K. Chem Res Toxicol 2006, 19, 356.
30. Roy. D. R.; Parthasarathi, R.; Maiti, B.; Subramanian, V.; Chattaraj, P. K. Bioorg Med Chem 2005, 13, 3405.
31. Parthasarathi, R.; Subramanian, V.; Roy. D. R.; Chattaraj, P. K. Bioorg Med Chem 2004, 12, 5533.
32. Padmanabhan, J.; Parthasarathi, R.; Subramanian, V.; Chattaraj, P. K. J Phys Chem A 2005, 109, 11043.
33. Padmanabhan, J.; Parthasarathi, R.; Subramanian, V.; Chattaraj, P. K. J Phys Chem A 2006, 110, 9900.
34. Zhang, Y.; Guo, Z.; You, X.-Z. J Am Chem Soc 2001, 123, 9378.
35. Costa, L. A. S.; Rocha, W. R.; De Almeida, W. B.; Dos Santos, H. F. J Chem Phys 2003, 118, 10584.
36. Lau, J. K. C.; Deubel, D. V. Chem—Eur J 2005, 11, 2849.
37. Baik, M. H.; Friesner, R.; Lippard, S. J. J Am Chem Soc 2003, 125, 14081.
38. Zimmermann, T.; Zeizinger, M.; Burda, J. V. J Inorg Biochem 2005, 99, 2184.
39. Raber, J.; Zhu, C. B.; Eriksson, L. A. J Phys Chem B 2005, 109, 11006.
40. Iczkowski, R. P.; Margrave, J. L. J Am Chem Soc 1961, 83, 3547.
41. Koopmans, T. A. Physica 1933, 1, 104.
42. Mendez, F.; Gazquez, J. L. J Am Chem Soc 1994, 116, 9298.
43. Yang, W.; Mortier, W. J. J Am Chem Soc 1986, 108, 5708.
44. Chattaraj, P. K.; Maiti, B.; Sarkar, U. J Phys Chem A 2003, 107, 4973.
45. Delley, B. J Chem Phys 1990, 92, 508.
46. Bock, C. W.; Trachtman, M. J Phys Chem 1994, 98, 95.
47. Gordon, M. S. Chem Phys Lett 1980, 76, 163.
48. Hehre, W. J.; Ditchfield, R.; Pople, J. A. J Chem Phys 1972, 56, 2257.
49. Becke, A. D. Phys Rev A 1988, 38, 3098.
50. Lee, C.; Wang, W.; Parr, R. G. Phys Rev 1988, 37, 785.
51. Tsuneda, T.; Suzumura, T.; Hirao, K. J Chem Phys 1999, 110, 10664.
52. Hamprecht, F. A.; Cohen, A. J.; Tozer, D. J.; Handy, N. C. J Chem Phys 1998, 109, 6264.
53. Hirshfeld, F. L. Theor Chim Acta 1977, 44, 129.
54. Andzelm, J.; Koelmel, C.; Klamt, A. J Chem Phys 1995, 103, 9312.
55. MATLAB. The Math Works, Inc.: Natick, USA.; 1999.
56. Penrose, R. Proc Cambridge Philos Soc 1955, 51, 406.
57. Milburn, G. H. W.; Truter, M. R. J Chem Soc A 1966, 1609.
58. Wysokiński, R.; Michalska, D. J Comput Chem 2001, 9, 901.
59. Soltzberg, L.; Margulis, T. M. J Chem Phys 1971, 55, 4907.
60. Beagley, B.; Cruickshank, D. W. J.; McAuliffe, C. A.; Pritchard, R. G.; Zaki, A, M.; Beddoes, R. L.; Cernik, R. J.; Mills, O. S. J Mol Struct 1985, 130, 97.
61. Bruck, M. A.; Bau, R.; Noji, M.; Inagaki, K.; Kidani, Y. Inorg Chim Acta 1984, 92, 279.
62. Spiegel, K.; Rothlisberger, U.; Carloni, P. J Phys Chem B 2004, 108, 2699.
63. Carloni, P.; Andreoni, W.; Hutter, J.; Curioni, A.; Giannozzi, P.; Parrinello, M. Chem Phys Lett 1995, 234, 50.
64. Parr, R. G.; Chattaraj, P. K. J Am Chem Soc 1991, 113, 1854.
65. Chattaraj, P. K.; Liu, G. H.; Parr, R. G. Chem Phys Lett 1995, 237, 171.
66. Screnci, D.; McKeage, M. J.; Galettis, P.; Hambley, T. W.; Palmer, B. D.; Baguley, B. C. Br J Cancer 2000, 82, 966.
67. Monti, E.; Gariboldi, M.; Maiocchi, A.; Marengo, E.; Cassino, C.; Gabano, E.; Osella, D. J Med Chem 2005, 48, 857.